AMERICAN JOURNAL OF BIOLOGY AND NATURAL SCIENCES
https://biojournals.us/index.php/AJBNS
**ISSN: 2997-7185**

Article

# Corrosion Behavior of Spray Pyrolysis–Deposited $BaTiO_3$, $SiO_2$, and $BaTiO_3/SiO_2$ Composite Coatings on Ti–13Nb–13Zr Alloy for dental implants

**Hamzah K. Rustam[1], Shanai M. Al-Bayati[2]**

1. MSc. In prosthodontic ministry of health, specialist dental center in Kirkuk
2. PhD in Prosthodontics College of medical Techniques University of AL-Kitab
*Correspondence: Hamzahdent89@gmail.com[1] , Shanai.mohamed@uoalkitab.edu.iq[2]

**Citation:** Rustam H. K., Al-Bayati S. M. hmed M. T., Corrosion Behavior of Spray Pyrolysis–Deposited $BaTiO_3$, $SiO_2$, and $BaTiO_3/SiO_2$ Composite Coatings on Ti–13Nb–13Zr Alloy for dental implants. American Journal of Biology and Natural Sciences 2026, 3(6), 146-157.

Received: 10th Mar 2026
Revised: 11th Apr 2026
Accepted: 20th May 2026
Published: 23th Jun 2026



**Abstract:** The long-term success of metallic implants depends on both corrosion resistance in physiological environments and strong osseointegration at the bone–implant interfaceIn, in this study Ti–13Nb–13Zr substrates were functionalized with $BaTiO_3$, $SiO_2$, and $BaTiO_3$–$SiO_2$ composite coatings deposited by spray pyrolysis. The rationale was to combine the piezoelectric stimulation of $BaTiO_3$ with the bioactive and surface-modifying properties of $SiO_2$ to achieve synergistic improvements in implant performance. Coatings were systematically optimized and characterized using XRD, EDX, FESEM test, and corrosion tests. The electrochemical corrosion test also achieved by measuring OCP, polarization curve tafel and EIS. Electrochemical tests revealed significantly lower corrosion current densities with higher polarization resistance for coated samples compared to the bare alloy, the $BaTiO_3$–$SiO_2$ composite showing the most stable electrochemical response. These findings indicate that spray-pyrolysed $BaTiO_3$–$SiO_2$ coatings provide a promising strategy to engineer multifunctional implant surfaces with superior corrosion protection and biological integration, advancing the design of next-generation load-bearing biomedical implants.in addition The result proves that the mixing between the two bioceramic combined the advantages of them and decreases the corrosion rate about 23 times; raise the protection efficiency to about 95%.

**Keywords:** Ti–13Nb–13Zr alloy; Spray pyrolysis; $BaTiO_3$ coatings; $SiO_2$ coatings; Corrosion resistance; piezoelectric biomaterials; Osseointegration.

## Introduction

Titanium and its alloys always have great interest to researchers in the field of biomedical applications [1,2]. Titanium and its alloy used for dental orthopedic implants and fixation [3,4]. Even they had an excellent corrosion resistance but still the fear from high accumulation of titanium itself or the additives in its alloys in human body has the major concern from researches those who dedicated themselves to conducting research to reduce the corrosion of these alloys [5,6,7]. One of the important titanium alloys which have attracted the attention of researchers in this field was Ti13Nb13Zr alloy

[8,9]. Researchers have resorted to several methods to reduce corrosion, such as surface treatment or applying various coating techniques. Many techniques was followed to coating biomaterials on biomedical alloys like electrophoretic deposition, dip coating, plasma sputtering, electrospining and pyrolysis spray[10,11,12,13]**.**The pyrolysis spray was a simple technique depending on principles of spraying the biomaterials as a solution on hot implant surface[14,15]. Many biomaterials ceramics has an interest to coat on biomedical metal and alloys like hydroxyapatite, titanium oxide, alumina and silicone oxide and barium titanate was one of those materials which have an important interest. Silicone oxide ($SiO_2$) often in the form of silica nanoparticles or silicon dioxide layers is widely used in medical implants due to its biocompatibility, inertness, and ability to improve the mechanical properties of biomedical devices [16,17,18,19,20]. It is frequently employed to enhance the surface characteristics and structural integrity of implants, particularly in orthopedics and dental applications. Barium titanate ($BaTiO_3$) is a lead-free, ferroelectric ceramic used in medical implants primarily for its piezoelectric properties, which mimic natural bone behavior to promote healing and tissue regeneration[21,22]. In this research we coat Ti13Nb13Zr alloy with SiO2, BaTiO3 and mixture of them using pyrolysis spray technique in order to investigate the enhancement of corrosion characteristics after coating. The coated samples tested by XRD, EDX, FESEM and the electrochemical corrosion also tested to evaluate the results.

**Materials and methods**

The Ti13NB13Zr alloy rod with 20 mm diameter with chemical composition shown in table (1) was cut with 2mm thickness using wire cutter machine. Then the samples were grinded with SiC grinding paper (p120-400) grit and cleaned with acetone (Sigma Aldrich, USA) twice using ultrasonic cleaner bath(Camel FSF030s, China). In order to prepare coating composite solution 1gm from polyvinylpyrolidone (PVP K30, CDH, India) was added to 10ml water in stirred vigorously for 20 minutes using magnetic stirrer (Alfa HS 860 , Iran). Then 40ml of absolute ethanol was added and stirred gently for 10 minutes, 3gm of $SiO_2$ (<30nm, Skyspring Nanomaterial, USA)was added to the previous solution and mixed gently for 10 minutes. The samples were coated using spray gun connected to (5 psi pressure) air compressor after preheating the samples to 80 °C on hot plate as shown in fig (***1*** and 2).The coated procedure was repeated to achieve two coated layers, then heat treated at 100 °C for one hour under air atmosphere using oven (Silver cryst, Germany).A second and third groups of Ti13NB13Zr alloy samples was coated with $BaTiO_3$ (<40nm, Skyspring Nanomaterial, USA) and mixed composite from $SiO_2$ and $BaTiO_3$with 50% of each one was used by same previous procedure of preparing composite solution and coating. The coated samples tested by XRD and EDX and FESEM.The electrochemical corrosion test also achieved by testing OCP, polarization curve tafel, and electrochemical impedance spectroscopy EIS to evaluate the results using potentiostat (CHI 604E, CHINA).The sample was connected as the working electrode, the graphite electrode as the counter electrode, and Ag/AgCl/KCl 3.5M electrode as the reference electrode as shown in fig (3), while the corrosion media was synthetic simulated bode fluid (SBF) with chemical composition listed in table (1).

**Table 1.** chemical composition of Ti13Nb13ZR alloy.

| **Chemical composition [% wt.]** | | | | | | | |
|---|---|---|---|---|---|---|---|
| **Nb** | **Zr** | **Fe** | **C** | **H** | **O** | **S** | **Ti** |
| **13.18** | **13.49** | **0.085** | **0.035** | **0.004** | **0.078** | **<0.001** | **balanced** |

**Table 2.** chemical composition of simulated body fluid (SBF) solution.[23]

| **ITEM** | **Reagent** | **Concentration g/l** |
|---|---|---|
| **1** | **8.035** | **NaCl** |
| **2** | **0.355** | **$NaHCO_3$** |
| **3** | **0.225** | **KCl** |
| **4** | **0.231** | **$K_2HPO_4$** |
| **5** | **0.311** | **$MgCl_2.6H_2O$** |
| **6** | **0.292** | **$CaCl_2$** |

| 7 | 0.072 | $Na_2SO_4$ |
|---|---|---|

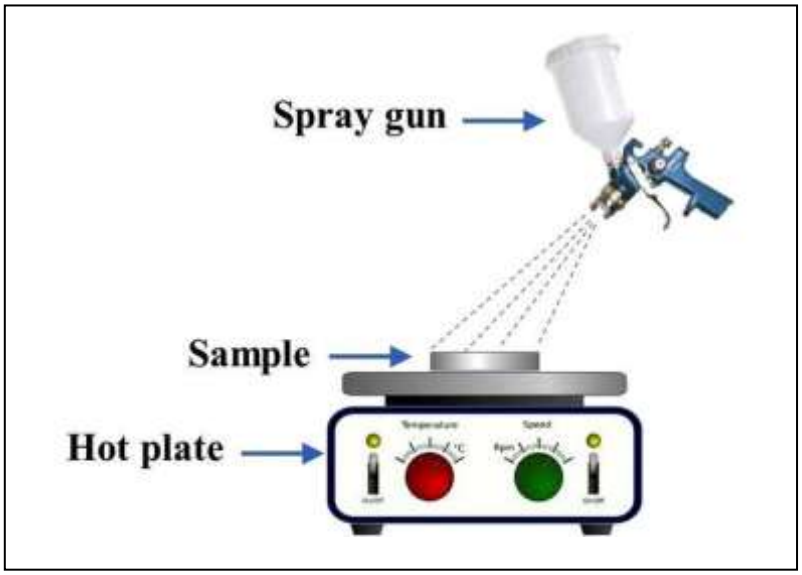


**Figure 1.** Simplified diagram for pyrolysis spray technique.

**Figure 2.** The pyrolysis spray system used for coating.

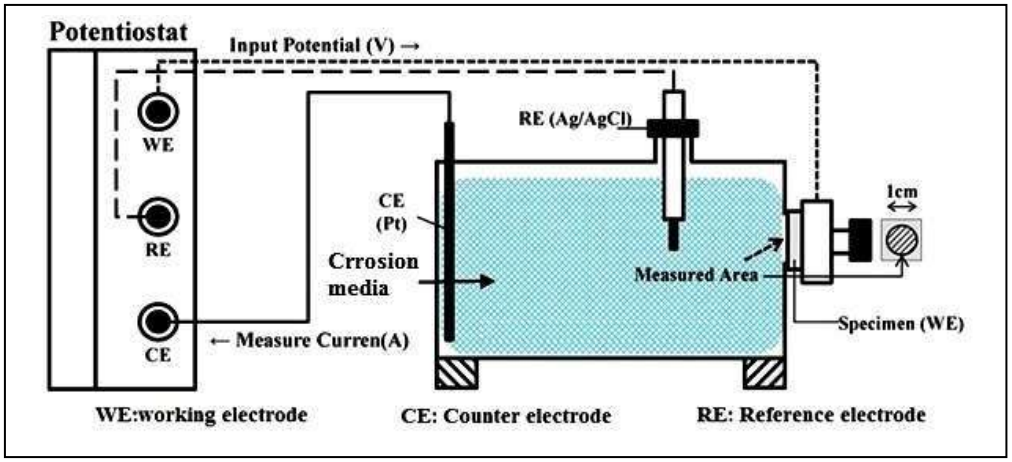


**Figure 3.** Schematic diagram for sample connection with potentiostat.

**Results and Discussion**

**Before immersing in SBF solution:**

**1-XRD test:**

The XRD pattern for Ti13Nb13Zr alloy uncoated sample in fig (4) shows a perfect matching with JCPDS no. 00-044-1294 for titanium at all peaks.

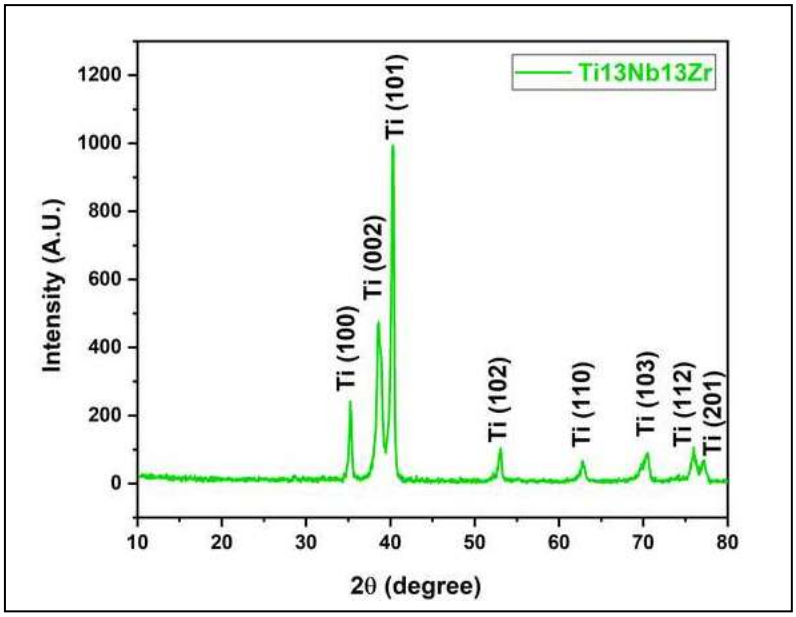


**Figure 4.** XRD pattern for Ti13Nb13Zr alloy uncoated sample.

The XRD pattern for Ti13Nb13Zr alloy sample coated with $SiO_2$ in fig (5) shows a good matching with JCPDS no. 00-0040-1498 at all peaks. Also we see the appearance of titanium peaks matching JCPDS no. 00-044-1294 as indicator of high porosity of coating layer and that happen due to the nature of $SiO_2$ which make very porous layer even it was nanoparticles.

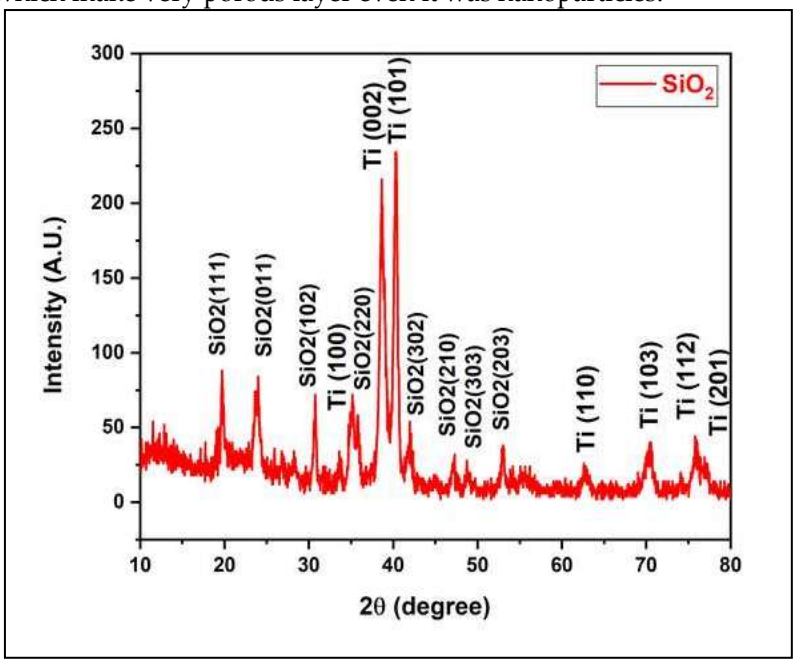


**Figure 5.** XRD pattern for Ti13Nb13Zr alloy sample coated with $SiO_2$ nanopowder.

The XRD pattern for Ti13Nb13Zr alloy sample coated with $BaTiO_3$ in fig (6) shows the appearance of BaTiO3 peaks matching JCPDS no.01-075-2116 with a few appearance of titanium peaks as indicator for good covering for coating layer.

The XRD pattern for Ti13Nb13Zr alloy sample coated with SiO2 and $BaTiO_3$ mixture shows the appearance of $SiO_2$ peaks matching JCPDS no. 00-0040-1498 and $BaTiO_3$ matching JCPDS no.01-075-2116 with no appearance for titanium peaks as an indicator for very good covering for coating layer. This happen because the $SiO_2$ Nano particles filled the porous between $BaTiO_3$ nanoparticles in coating layer.

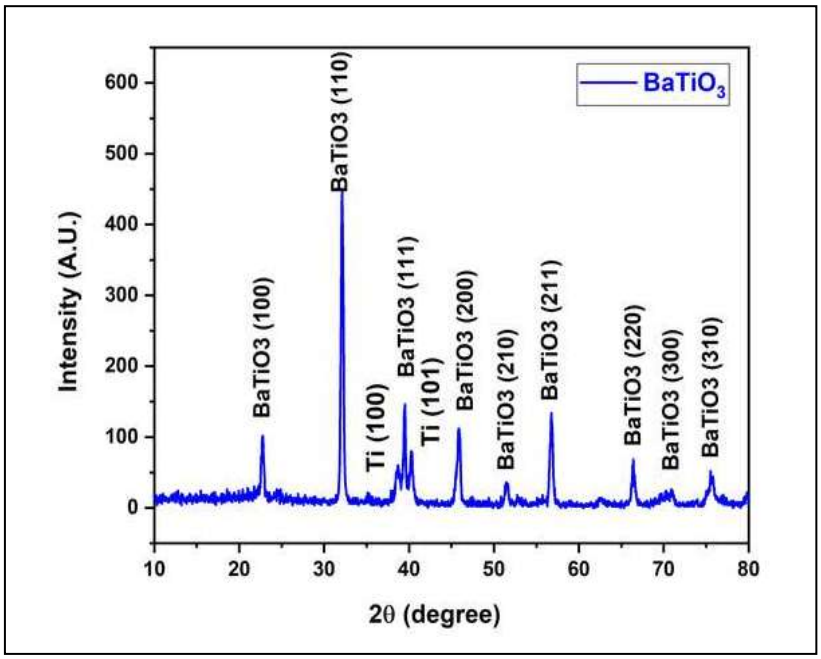


**Figure 6.** XRD pattern Ti13Nb13Zr alloy sample coated with $BaTiO_3$naopaowder.

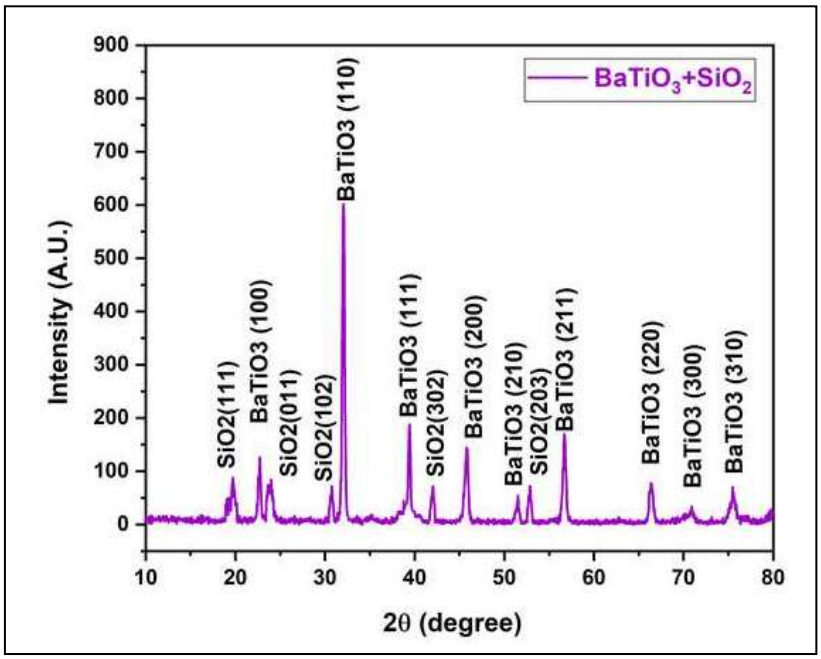


**Figure 7.** XRD pattern Ti13Nb13Zr alloy sample coated withSiO2 and $BaTiO_3$naopaowder mixture.

2- **EDX test:**

The EDX elemental analysis for uncoated Ti13Nb13Zr alloy shows the appearance of composition element at concentrations similar to those supplied by the manufacturer as shown in fig (8).

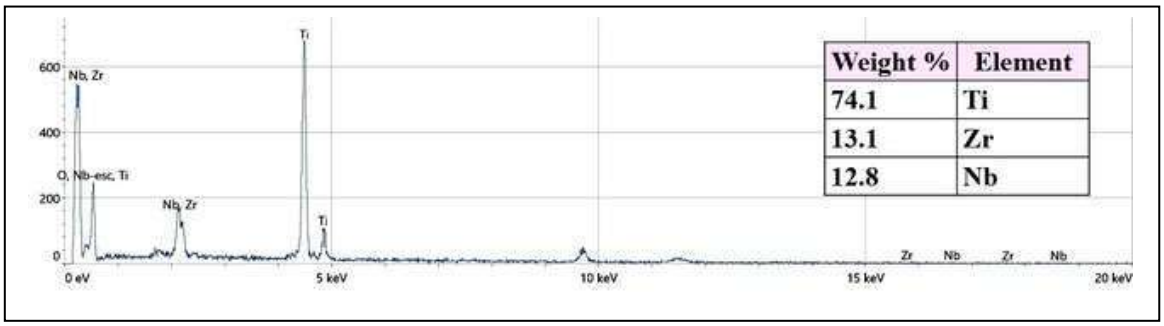


| Weight % | Element |
|---|---|
| 74.1 | Ti |
| 13.1 | Zr |
| 12.8 | Nb |

**Figure 8.** EDX elemental analysis for uncoated Ti13Nb13Zr alloy.

The EDX elemental analysis for sample coated with $SiO_2$ in fig (9) shows the appearance of silicon and oxygen mainly from $SiO_2$. The appearance of carbon came from PVP polymer. Also we see little appearance of titanium because the porosity in coating layer.

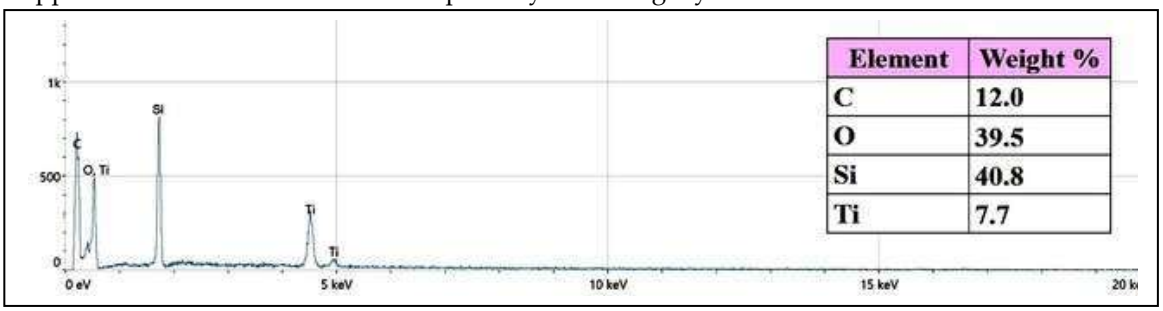


| Element | Weight % |
|---|---|
| C | 12.0 |
| O | 39.5 |
| Si | 40.8 |
| Ti | 7.7 |

**Figure 9.** EDX elemental analysis for Ti13Nb13Zr alloy coated with $SiO_2$.

The EDX elemental analysis for sample coated with $BaTiO_3$ in fig (10) shows the appearance of barium, titanium and oxygen mainly from $BaTiO_3$. The appearance of carbon came from PVP polymer.

The EDX elemental analysis for sample coated with SiO2 and $BaTiO_3$ mixture in fig (11) shows the appearance of silicone, barium, titanium and oxygen mainly from SiO2 and $BaTiO_3$. The appearance of carbon came from PVP polymer.

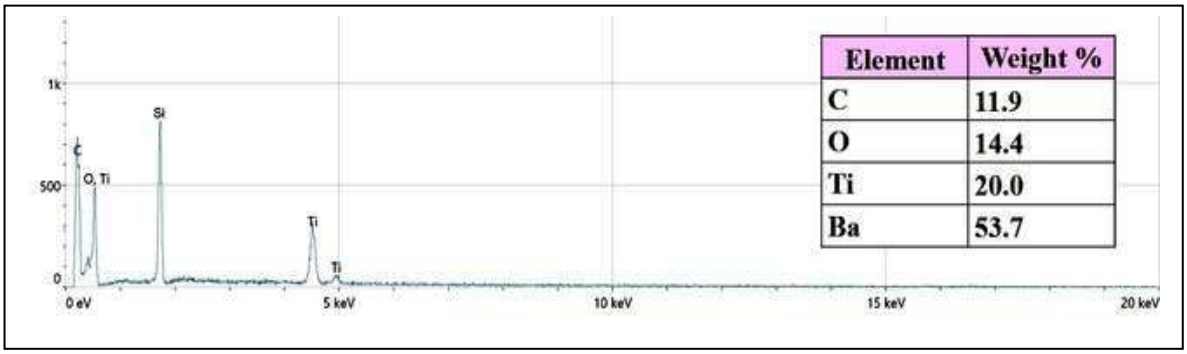


| Element | Weight % |
|---|---|
| C | 11.9 |
| O | 14.4 |
| Ti | 20.0 |
| Ba | 53.7 |

**Figure 10.** EDX elemental analysis for Ti13Nb13Zr alloy coated with $BaTiO_3$.

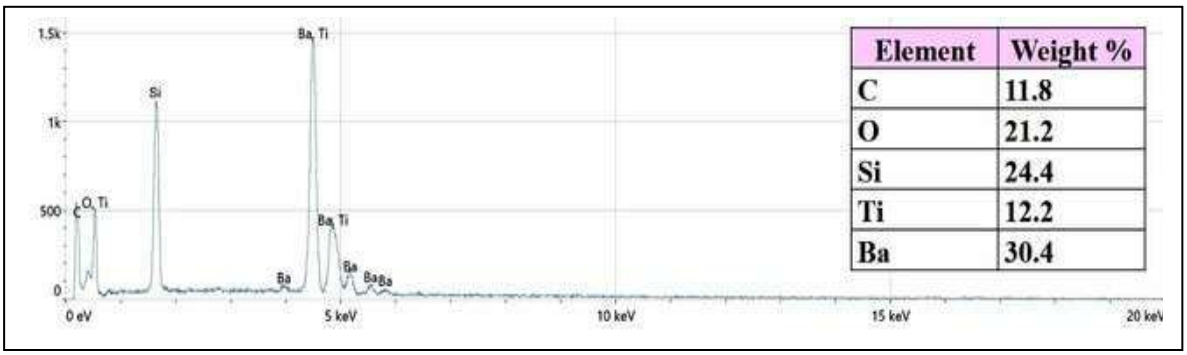


| Element | Weight % |
|---|---|
| C | 11.8 |
| O | 21.2 |
| Si | 24.4 |
| Ti | 12.2 |
| Ba | 30.4 |

**Figure 11.** EDX elemental analysis for Ti13Nb13Zr alloy coated with SiO2 and $BaTiO_3$ mixture.

**3-FESEM test:**

The FESEM test images for all samples in fig (12: a-h) show high agglomeration and cracks and high porosity in the $SiO_2$ coated sample layer this was due to nature of $SiO_2$ crystals. The sample coated with $BaTiO_3$ shows very uniform coated layer with no agglomeration or cracks with no porosity but the high magnification picture shows a nano scale cracks. The mixed ceramics coated layer images shows a characteristic between $SiO_2$ sample and $BaTiO_3$ sample, where the agglomeration and cracks was appear but more less than $SiO_2$ coated sample the coated was uniform but the high magnification picture shows high porosity than BaTiO3 coated sample and less than $SiO_2$ sample. The particle size for $SiO_2$ coated sample varied between (83.74-136.1) nm, for $BaTiO_3$ coated sample varied between (36.99 – 53.64) nm and for mix coated sample varied between (22.91-60.9) nm, i.e. this ensure that SiO2 affect the nature of coated layer causing more agglomeration.

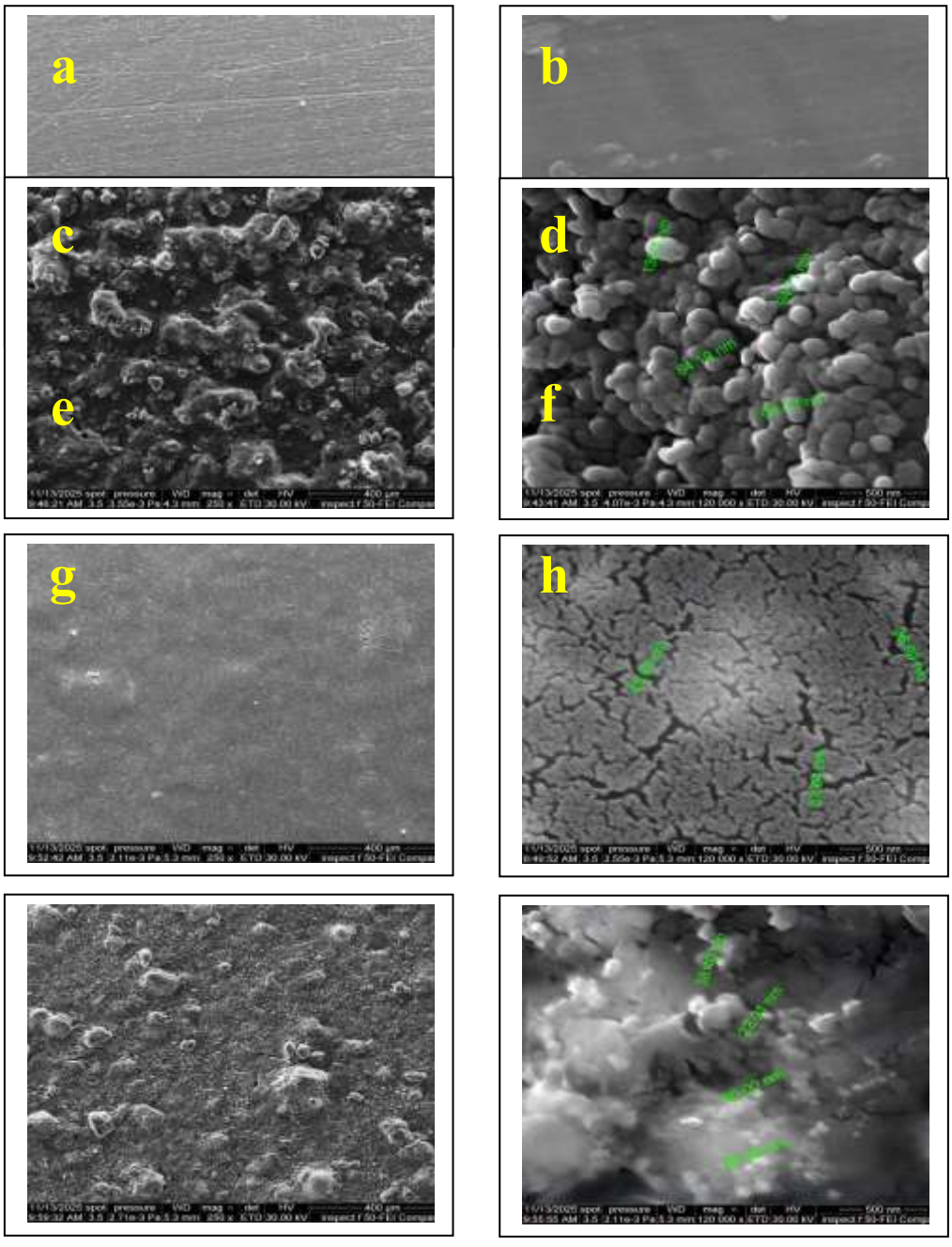

**Figure 12.** FESEM test images for all samples in different magnifications (a,b): uncoated, (c,d) :$SiO_2$ coated, (e.f): $BaTiO_3$ coated,(g,h): mix coated.

**4-Electrochemical corrosion test:**

The open circuit test shows increasing in passivation especially in the sample coated with mixture of $SiO_2$ and BaTiO3where the OCP reach to -0.29 V compared with -0.655 V for uncoated sample as shown in fig (13) and table (3).

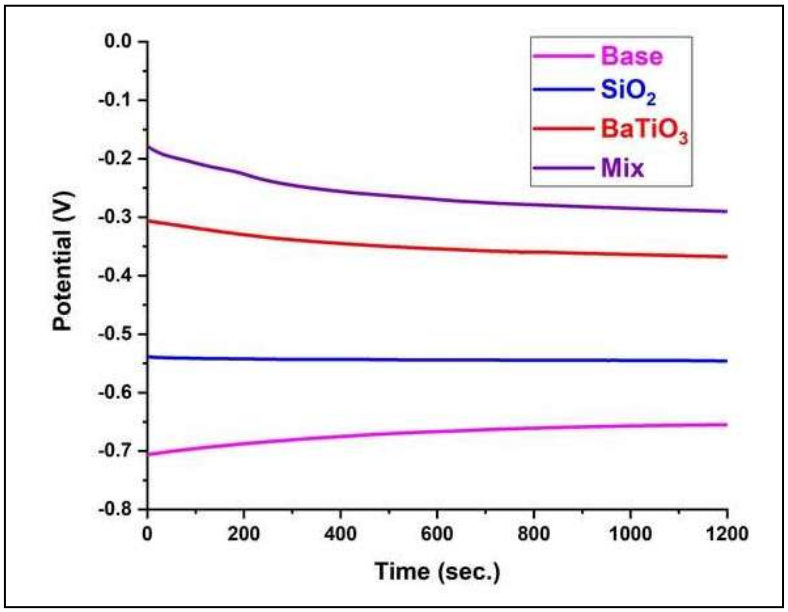


**Figure 13.** OCP test comparison for all samples.

**Table 3.** OCP test results for all samples.

| ITEM | OCP (V) |
|---|---|
| Base | -0.655 |
| $SiO_2$ | -0.545 |
| $BaTiO_3$ | -0.367 |
| Mix | -0.290 |

The polarization curve test (tafel) show decreasing in corrosion rate reach to $1.610\times10^{-4}$ mmpy compared with $3.785\times10^{-3}$ mmpy for uncoated sample, i.e. the corrosion rate decreased 23 times as shown in fig (14) and table (4).

The protection efficiency can be calculated from the following equation:

$$PE\% = \frac{icorr.uncoated - icorr.\ coated}{icorr.\ uncoted} \times 100 \ldots\ldots.[24]$$

We see from table (5) that the protection efficiency increased and reached to 95.74% for sample coated with mix ceramics and that an excellent result.

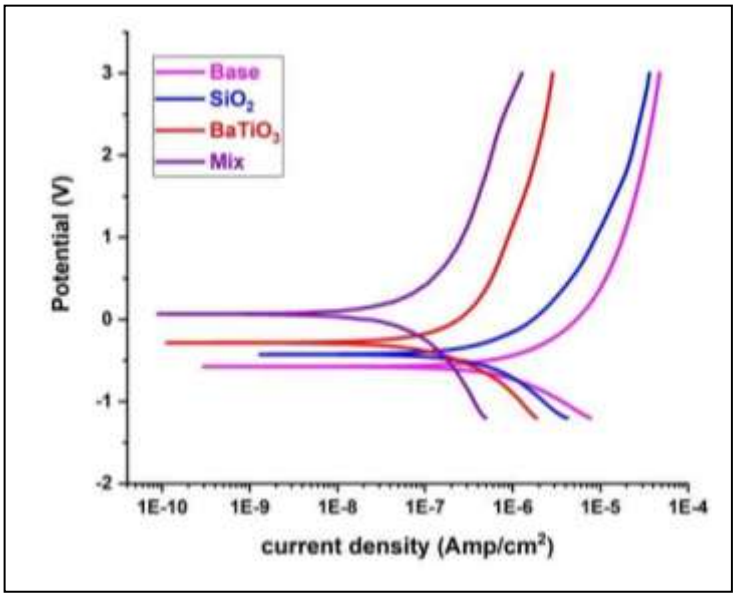


**Figure 14.** polarization curve tafel comparison for all samples.

**Table 4.** corrosion characteristics for all samples.

| ITEM | Icorr. (Amp) | protection efficiency % |
|---|---|---|
| Base | $4.224\times10^{-7}$ | ------- |
| $SiO_2$ | $1.442\times10^{-7}$ | 65.86 |
| $BaTiO_3$ | $6.075\times10^{-8}$ | 85.61 |
| Mix | $1.797\times10^{-8}$ | 95.74 |

**Table 5.** calculated protection efficiency for all coated samples.

| ITEM | Icorr. (Amp) | Corrosion rate (mmpy) |
|---|---|---|
| Base | $4.224\times10^{-7}$ | $3.785\times10^{-3}$ |
| $SiO_2$ | $1.442\times10^{-7}$ | $1.292\times10^{-3}$ |
| $BaTiO_3$ | $6.075\times10^{-8}$ | $5.443\times10^{-4}$ |
| Mix | $1.797\times10^{-8}$ | $1.610\times10^{-4}$ |

The electrochemical impedance spectroscopy test (EIS) was achieved for uncoated sample and the result coated sample which was that coated with $SiO_2$ and $BaTiO_3$. The uncoated sample shows a typical randles circuit equivalent circuit as shown in fig (15) while the sample coated with $SiO_2$ and $BaTiO_3$ shows an equivalent circuit for porous layer as shown in fig (16). The comparison between the uncoated and coated sample shows the great difference in resistance as shown in fig (17).

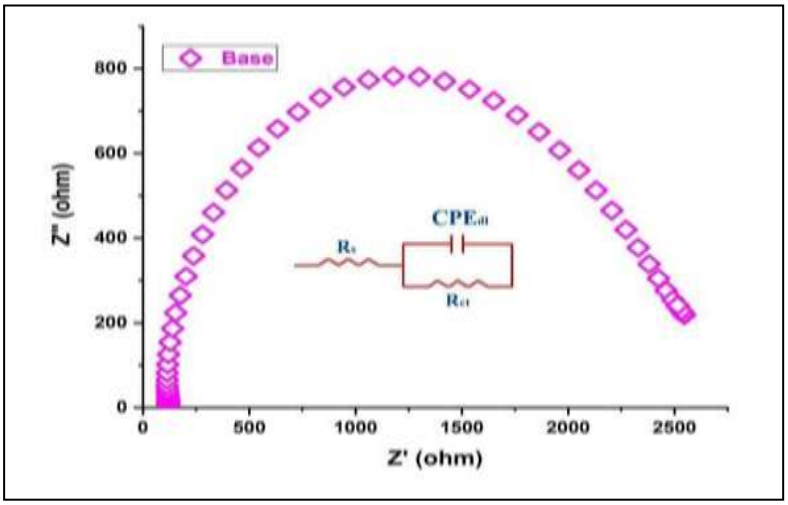

**Figure 15.** EIS test for uncoated sample with the equivalent circuit used for fitting the curve.

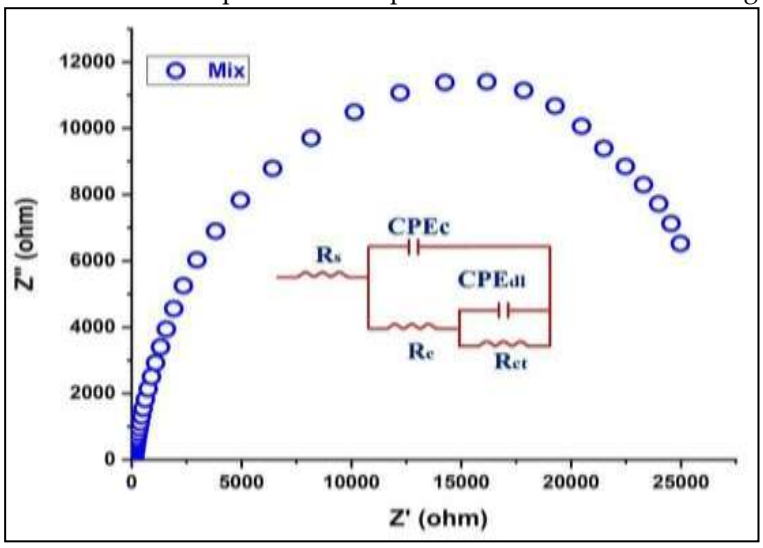


**Figure 16.** EIS test for sample coated with $SiO_2$ and $BaTiO_3$with the equivalent circuit used for fitting the curve.

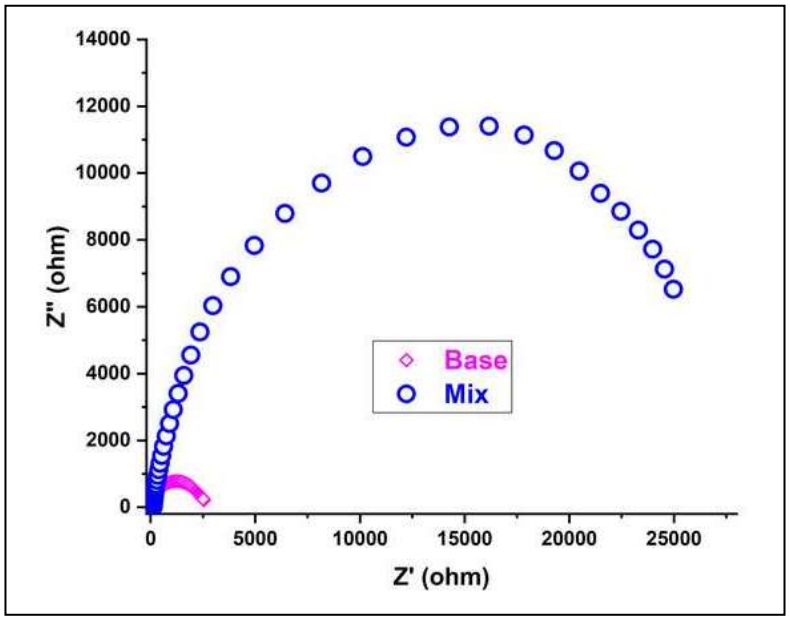


**Figure 17.** EIS test comparison between uncoated and mix coated sample.

The extracted parameters from fitting the two samples in table (6) shows increasing in total resistance to 24346 (ohm) for sample coated with mix ceramics compared with 2713 (ohm) for uncoated sample, i.e. the resistance increased about 9 times. Also we see the resistance for coating layer was for sample coated with mix ceramics was 23200 ohm this indicated the coating cause the increasing in resistance value.

**Table 6.** extracted parameters from fitting the two samples

| Parameters | Uncoated | Mix coated |
|---|---|---|
| $R_S$ (ohm) | 101 | 98 |
| $R_C$(ohm) | ----- | 23200 |
| $R_{dl}$(ohm) | 2612 | 3048 |
| $CPE_C$(F) | ----- | 3.7586E-04 |

| | | |
|---|---|---|
| n1 | ----- | 0.997 |
| $CPE_{dl}$(F) | 3.7221E-06 | 2.2116E-06 |
| n2 | 0.96469 | 0.939 |
| Rtotal (ohm) | 2713 | 24346 |

**Conclusion:**

From previous results we can conclude that the coating with $SiO_2$ and $BaTiO_3$mix ceramics combined the advantages of the two materials and produced a coating layer with high resistance to corrosion , where it was achieved 23 times reduction in corrosion and has a resistance about 9 times than uncoated sample.

**REFERENCES**


[1] GBD 2021 Antimicrobial Resistance Collaborators, "Global burden of bacterial antimicrobial resistance 1990–2021: A systematic analysis with forecasts to 2050," *Lancet*, vol. 404, no. 10459, pp. 1199–1226, 2024.

[2] Antimicrobial Resistance Collaborators, "Global burden of bacterial antimicrobial resistance in 2019: A systematic analysis," *Lancet*, vol. 399, no. 10325, pp. 629–655, 2022.

[3] World Health Organization, *WHO Bacterial Priority Pathogens List, 2024: Bacterial Pathogens of Public Health Importance to Guide Research, Development and Strategies to Prevent and Control Antimicrobial Resistance*. Geneva, Switzerland: World Health Organization, 2024.

[4] E. Tacconelli, E. Carrara, A. Savoldi, S. Harbarth, M. Mendelson, D. L. Monnet, *et al*., "Discovery, research, and development of new antibiotics: The WHO priority list of antibiotic-resistant bacteria and tuberculosis," *Lancet Infectious Diseases*, vol. 18, no. 3, pp. 318–327, 2018.

[5] A. Y. Peleg, H. Seifert, and D. L. Paterson, "Acinetobacter baumannii: Emergence of a successful pathogen," *Clinical Microbiology Reviews*, vol. 21, no. 3, pp. 538–582, 2008.

[6] B. A. Evans and S. G. B. Amyes, "OXA β-lactamases," *Clinical Microbiology Reviews*, vol. 27, no. 2, pp. 241–263, 2014.

[7] L. Poirel and P. Nordmann, "Carbapenem resistance in Acinetobacter baumannii: Mechanisms and epidemiology," *Clinical Microbiology and Infection*, vol. 12, no. 9, pp. 826–836, 2006.

[8] G. Mancuso, A. Midiri, E. Gerace, and C. Biondo, "Bacterial antibiotic resistance: The most critical pathogens," *Pathogens*, vol. 10, no. 10, Art. no. 1310, 2021.

[9] J. Strahilevitz, G. A. Jacoby, D. C. Hooper, and A. Robicsek, "Plasmid-mediated quinolone resistance: A multifaceted threat," *Clinical Microbiology Reviews*, vol. 22, no. 4, pp. 664–689, 2009.

[10] A. Robicsek, G. A. Jacoby, and D. C. Hooper, "The worldwide emergence of plasmid-mediated quinolone resistance," *Lancet Infectious Diseases*, vol. 6, no. 10, pp. 629–640, 2006.

[11] G. A. Jacoby, J. Strahilevitz, and D. C. Hooper, "Plasmid-mediated quinolone resistance," *Microbiology Spectrum*, vol. 2, no. 5, Art. no. PLAS-0006-2013, 2014.

[12] A. P. Magiorakos, A. Srinivasan, R. B. Carey, Y. Carmeli, M. E. Falagas, C. G. Giske, *et al*., "Multidrug-resistant, extensively drug-resistant and pandrug-resistant bacteria: An international expert proposal for interim standard definitions for acquired resistance," *Clinical Microbiology and Infection*, vol. 18, no. 3, pp. 268–281, 2012.

[13] Clinical and Laboratory Standards Institute, *Performance Standards for Antimicrobial Susceptibility Testing*, 36th ed., CLSI Supplement M100. Wayne, PA, USA: Clinical and Laboratory Standards Institute, 2026.

[14] S. A. Bustin, V. Benes, J. A. Garson, J. Hellemans, J. Huggett, M. Kubista, *et al*., "The MIQE guidelines: Minimum information for publication of quantitative real-time PCR experiments," *Clinical Chemistry*, vol. 55, no. 4, pp. 611–622, 2009.

[15] K. Tamura, G. Stecher, and S. Kumar, "MEGA11: Molecular Evolutionary Genetics Analysis version 11," *Molecular Biology and Evolution*, vol. 38, no. 7, pp. 3022–3027, 2021.

[16] N. Saitou and M. Nei, "The neighbor-joining method: A new method for reconstructing phylogenetic trees," *Molecular Biology and Evolution*, vol. 4, no. 4, pp. 406–425, 1987.

[17] D. W. Hosmer, S. Lemeshow, and R. X. Sturdivant, *Applied Logistic Regression*, 3rd ed. Hoboken, NJ, USA: John Wiley & Sons, 2013.

[18] M. Afsharian, S. Vaziri, A. Janbakhsh, F. Mansouri, B. Sayad, F. Hamzavi, *et al*., "The abundance of plasmid-mediated quinolone resistance genes in Enterobacter cloacae strains isolated from clinical specimens in Kermanshah, Iran," *Canadian Journal of Infectious Diseases and Medical Microbiology*, vol. 2024, Art. no. 8849097, 2024.

[19] J. J. Wu, W. C. Ko, S. H. Tsai, and J. J. Yan, "Prevalence of plasmid-mediated quinolone resistance determinants QnrA, QnrB, and QnrS among clinical isolates of Enterobacter cloacae in a Taiwanese hospital," *Antimicrobial Agents and Chemotherapy*, vol. 51, no. 4, pp. 1223–1227, 2007.

[20] M. F. Al-Marjani, K. A. Kadhim, and A. B. Mohammed, "The context of blaOXA-23 gene in Iraqi carbapenem-resistant Acinetobacter baumannii isolates belonging to global clone 1 and global clone 2," *Infection and Drug Resistance*, vol. 17, pp. 4385–4396, 2024.

[21] H. O. Hashim and M. B. S. Al-Shuhaib, "Detection of carbapenemase genes in Acinetobacter baumannii isolates from Al-Azizya Hospital, Wasit, Iraq," *Jundishapur Journal of Microbiology*, vol. 18, no. 2, Art. no. e159737, 2025.

[22] P. G. Higgins, C. Dammhayn, M. Hackel, and H. Seifert, "Global spread of carbapenem-resistant Acinetobacter baumannii," *Journal of Antimicrobial Chemotherapy*, vol. 65, no. 2, pp. 233–238, 2010.

[23] P. Nordmann and L. Poirel, "Epidemiology and diagnostics of carbapenem resistance in Gram-negative bacteria," *Clinical Infectious Diseases*, vol. 69, Suppl. 7, pp. S521–S528, 2019.

[24] D. C. Hooper and G. A. Jacoby, "Mechanisms of drug resistance: Quinolone resistance," *Annals of the New York Academy of Sciences*, vol. 1354, no. 1, pp. 12–31, 2015.

[25] M. Kafshnouchi, M. Safari, A. Khodavirdipour, A. Bahador, S. H. Hashemi, M. S. Alikhani, *et al*., "Molecular detection of blaOXA-type carbapenemase genes and antimicrobial resistance patterns among clinical isolates of Acinetobacter baumannii," *Global Medical Genetics*, vol. 9, no. 2, pp. 118–123, 2022.

[26] World Health Organization, *Global Antimicrobial Resistance and Use Surveillance System (GLASS) Report 2022*. Geneva, Switzerland: World Health Organization, 2022.

[27] F. Firoozeh, Z. Mahluji, A. Khorshidi, and M. Zibaei, "Molecular characterization of class 1, 2 and 3 integrons in clinical multidrug-resistant Enterobacter cloacae isolates," *Antimicrobial Resistance and Infection Control*, vol. 8, Art. no. 59, 2019.

[28] L. Dijkshoorn, A. Nemec, and H. Seifert, "An increasing threat in hospitals: Multidrug-resistant Acinetobacter baumannii," *Nature Reviews Microbiology*, vol. 5, no. 12, pp. 939–951, 2007.